APPLIED ORGANOMETALLIC CHEMISTRY, VOL. 12, 121–128 (1998)

Investigation of MMT Adsorption on Soils by Diffuse Reflectance Infrared Spectroscopy (DRIFTS) and Headspace Analysis Gas-phase Infrared Spectroscopy (HAGIS)

Andrew J. Vreugdenhil[1] and Ian S. Butler[2]*
[1] Department of Mining and Metallurgical Engineering, McGill University, 3610 University Street, Montreal, Quebec, Canada H3A 2B2
[2] Department of Chemistry, McGill University, 801 Sherbrooke Street West, Montreal, Quebec, Canada H3A 2K6

Diffuse reflectance infrared Fourier-transform spectroscopy (DRIFTS) and headspace analysis gas-phase infrared spectroscopy (HAGIS) were used to investigate interactions between soils and the gasoline additive methylcyclopentadienylmanganese tricarbonyl (MMT). Various soil samples, as well as alumina and silica substrates, were studied. Each substrate exhibited a splitting or broadening of the degenerate *e* ν(CO) band of MMT, suggesting an interaction involving one or two of the CO ligands. The adsorption was shown to be reversible under relatively mild conditions using HAGIS. The proposed interaction is of the Brønsted type, involving the carbonyl oxygen and a surface-bound water or hydroxyl group. This type of interaction could stabilize MMT by inhibiting photoejection of CO ligands, a common first step in the decomposition of organometallic carbonyl compounds such as MMT. © 1997 John Wiley & Sons, Ltd.

Appl. Organometal. Chem. **11**, 121–128 (1998)

Keywords: MMT; soils; interactions; Fourier-transform IR

Received 1 May 1997; accepted 11 August 1997

† Correspondence to: Ian S. Butler, Department of Chemistry, McGill University, 801 Sherbrooke Street West, Montreal, Quebec, Canada H3A 2K6.
Email addresses: I. S. Butler (Butler@omc.lan.mcgill.ca), A. J. Vreugdenhil (AndrewV@minmet.lan.mcgill.ca)

INTRODUCTION

Methylcyclopentadienylmanganese tricarbonyl (MMT) was introduced in the 1950s as a second antiknock agent for leaded fuels. The mechanism of its antiknock behaviour is somewhat unusual[1] and it has a synergistic effect when used with tetraethyl-lead (TEL). It is also used as a smoke suppressant in fuel oil for turbines and boilers at concentrations between 6.5 and 130 mg Mn l^{-1}. It has been marketed as a primary antiknock agent since 1974.[2] Canada approved the use of MMT as a primary antiknock agent at concentrations up to 18 mg Mn l^{-1} in unleaded gasoline in the mid-1970s.[3] After an extensive series of court cases, the Environmental Protection Agency in the USA was required to remove a ban on the use of MMT.[4]

When MMT was introduced for use as a primary antiknock agent in gasoline, it was considered to be a safe replacement for TEL because its decomposition products are the comparatively safe manganese oxides, rather than lead oxides. However, some concerns have been raised over the physiological impacts of manganese and its compounds. Toxicological and epidemiological studies have been performed on inorganic forms of manganese. Advanced manganese poisoning is described in a syndrome known as 'manganism'. Manganese poisoning occurs in two stages. The first is reversible and is characterized by psychological disturbances. The second stage is an irreversible neurological disturbance with symptoms resembling Parkinson's syndrome. Manganism has been identified in all industries associated with the production and use of manganese involving high concentrations of manganese dusts and

 CCC 0268–2605/98/020121–08 $17.50

fumes.[5]

As a lypophillic organometallic complex, MMT can be absorbed into the body by a number of pathways. It can be readily absorbed through the skin, the enteric tract and the lungs.[2] In studies of acute exposure, MMT caused tremors, slowed respiration and led to terminal coma in a wide variety of species. Oral LD_{50} values for rats varied between 8 and 176 mg kg^{-1} depending on the preparation.[2,6] This is significantly more toxic than inorganic forms of manganese. Studies of chronic exposure of dogs, cats, rabbits and other species to MMT have shown damage to the liver and kidneys at gas-phase exposures between 14 and 17 mg m^{-3}. However, all animals survived 150 daily exposures to 6.4 mg m^{-3} without significant effect or pathological change.[2]

Combustion of MMT in gasoline is considered to be 98.7% complete in an internal combustion engine.[7] The environmental half-life for free airborne MMT is suggested to be about 15 s, as it would be rapidly photolysed.[3,7] However, our studies have shown that, when introduced to soils, MMT can be stabilized for extended periods and its environmental half-life may be lengthened dramatically.[8] Metal carbonyls and other organometallic complexes similar to MMT have been shown to adsorb readily to high-surface-area materials and are studied widely in the area of heterogeneous catalysis using a variety of IR spectroscopic techniques.[9]

The results of a study investigating this enhanced stability are presented here. Four different soils as well as alumina and silica were used as substrates for MMT adsorption. The splittings and frequencies of the IR bands assigned to the CO ligands of adsorbed MMT were used to probe the interaction between the adsorbate and the various surfaces. The thermal reversibility of the interaction was also investigated using an *in-situ* headspace analysis gas-phase infrared technique.

EXPERIMENTAL

Methylcyclopentadienylmanganese tricarbonyl (MMT, AK-33X, HiTec2000; Ethyl Corporation, Baton Rouge, FL, USA) was distilled under nigtrogen, and stored frozen until needed. All solvents employed were spectrograde quality and were used as received. Sterilized, all-purpose topsoil was purchased from the Gardening Centre of the downtown Montreal Eaton department store and was used as received. All other soil samples were obtained from Agriculture Canada (Centre for Land and Biological Resources Research). They were standard soils, exhibiting a range of physical and chemical characteristics (pH, cation-exchange capacity, percentage of organic carbon, percentage of clay, etc) according to standard soil-analysis methods. A summary of the relevant characteristics is presented in Table 1.

Table 1 Characteristics of the soils investigated

Soil	pH	Organic carbon (%)	Clay (%)
ECSS2	4.4	5.4	3
ECSS4	8.2	0.2	12
ECSS5	6.6	2.9	26
ECSS8	7.6	1.3	28

Alumina (Aldrich standard grade, neutral and basic 150-mesh) and silica (Aldrich Davisil, grade 644, 100–200-mesh) were used as model surfaces for comparison with the soils. Grades II–V of basic and neutral alumina were prepared according to standard procedures.[10] The silica was used as received.

The DRIFTS data for the solid samples were recorded on a Bruker IFS-88 FT spectrometer with an extended interferometer and an on-axis ellipsoidal mirror, diffuse reflectance accessory (Spectra-Tech, Inc.). The instrument was equipped with an MCT detector cooled by liquid nitrogen. Unless otherwise indicated, the spectra were measured at 4 cm^{-1} resolution and, typically, 1000 scans were co-added. Kubelka–Munk and $\log(1/R)$ spectra were obtained by ratioing the resulting spectra against the spectrum of a crushed KBr background. High- (0.11 cm^{-1}) and medium-resolution (4 cm^{-1}) gas-phase spectra of MMT were obtained by using a 10-cm pathlength cell on the same instrument. The solution IR spectra were collected at 4 cm^{-1} resolution with the aid of a 1.00-mm solution cell fitted with KBr windows on a Bruker IFS-48 FT spectrometer equipped with a room-temperature deuterium triglycine sulfate (DTGS) detector.

Preparation of samples was carried out as follows. MMT solutions in hexanes were placed in a beaker with a known amount of adsorbate (soil, alumina or silica). These samples were then

allowed to dry in air. The samples were diluted to between 1 and 5% in infrared-grade KBr powder and DRIFT spectra were acquired. Variable-loading experiments were performed by using different concentrations of MMT in the hydrocarbon solutions applied to the surface under investigation.

Spectral analysis

Peak-fitting analysis was performed using the Bruker OPUS 2.0 spectral acquisition and analysis software. Two approaches were attempted. The first involved subtraction of a DRIFT spectrum of the appropriate blank substrate from the MMT-loaded substrate. The remaining spectral components due to the carbonyl stretches of MMT were peak-fitted (Levenberg–Marquardt optimization[11]). However, the variations in relative peak intensity across the DRIFT spectrum made this approach unacceptably arbitrary. The second approach involved a two-step peak-fitting process. Those IR bands that appear in the region of interest (2150–1800 cm^{-1}) in the blank substrate were subjected to a peak fit. This model of the background peaks was then used to account for the background peaks appearing in the DRIFT spectrum of the substrate after it had been treated with MMT. Peaks corresponding to the CO stretches of the MMT were added to the model. No variation in the frequency, peak shape or peak width of the background peaks was expected, so these characteristics of the background peaks were not allowed to change. The intensity of these peaks was left unconstrained to allow for differences in sample packing, instrument throughput and analyte/KBr dilution ratios as described above. All of the parameters of the peaks corresponding to the CO stretches of MMT were allowed to vary. Using this process, all of the peak-fit models resulted in a residual root-mean-square (RMS) error of less than 2%. The models were found to be highly reproducible. This second peak-fitting method was used for all analyses presented in this paper.

RESULTS AND DISCUSSION

In solution, the IR spectra of MMT exhibit two ν(CO) bands. Considering just the local C_{3v} symmetry of the manganese tricarbonyl moiety, these two bands are assigned to a_1 and e CO stretching modes. The symmetric a_1 stretching mode appears around 2020 cm^{-1} whereas the doubly degenerate e mode is located near 1935 cm^{-1}.[12] The exact frequencies and peak widths depend on the polarity of the solvent. A summary of the observed ν(CO) frequencies in selected organic solvents is presented in Table 2 and they are consistent with published values.[12, 13, 18] The ν(CO) frequencies of MMT and, particularly, the e mode, are sensitive to the chemical environment of the molecule.

Table 2 CO stretching frequencies for MMT in various solvents and in the gas phase

	ν(CO) (cm^{-1})	
Solvent	a_1	e
Tetrahydrofuran	2016.2	1929.3
Cyclohexane	2022.0	1939.2
Octane	2024.4	1942.3
Gas phase	2036.8	1960.6

Earlier work in our laboratory has shown that MMT is readily adsorbed onto soil surfaces and is retained there for long periods of time.[8] As illustrated in Fig. 1, DRIFT spectra of soils and surfaces treated with MMT exhibit additional peaks in the ν(CO) region (2150–1800 cm^{-1}). These observed bands are consistent with the ν(CO) a_1 and e modes expected for MMT in

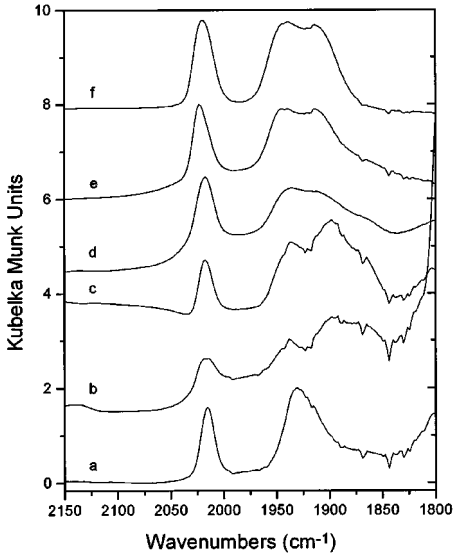

Figure 1 DRIFT spectra [ν(CO) region] of MMT adsorbed on (a) topsoil, (b) soil ECSS4, (c) soil ECSS5, (d) soil ECSS8, (e) silica and (f) alumina.

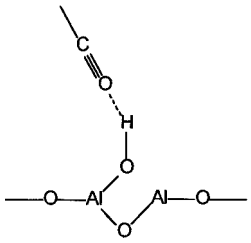

Figure 2 Proposed Brønsted interaction site for MMT adsorption.

various chemical environments. The soil sample ECSS2 did not retain an amount of MMT that is detectable using DRIFTS. This soil sample was unique in two of its characteristics: it was the only soil that had an acidic pH and it was the soil with the lowest clay component (3% versus 12% and above). The fact that ECSS2 has a low clay content could be an important factor in its ability to retain MMT, as the binding site proposed in the following discussion is an inorganic clay-like site rather than an organic site (Fig. 2).

Upon closer examination of the spectra in Fig. 1, the lower-energy *e*-mode peak is split or broadened considerably for each of the surfaces. The largest splitting is observed for the soils ECSS5 (trace c) and ECSS4 (trace b). ECSS8 (trace d) and the topsoil (trace a) do not show a complete splitting of the band but the *e* mode is broad and asymmetrical. Since the soils all contain a variety of functional groups, it was decided to investigate the adsorption of MMT on less complex substrates for comparison. To this end, alumina and silica were studied as substrates for MMT absorption. The ν(CO) regions of the DRIFT spectra of MMT on alumina and silica are also presented in Fig. 1. Alumina and silica also cause a splitting in the ν(CO) *e* mode of MMT of the order of that observed for the soils ECSS5 and ECSS4, although the band positions are at slightly higher energies.

The broadening or splitting of the *e* mode is consistent with a breakdown in the local C_{3v} symmetry of the $Mn(CO)_3$ moiety. If one of the carbonyl ligands interacts with the surface to a greater extent than do the others, the local symmetry would decrease to C_s symmetry. Under this lower symmetry, the *e* mode should split into two nondegenerate modes, $a'(2)$ and a''. Earlier high-resolution gas-phase IR studies of MMT have shown discrepancies in the rotational fine structure of the *e* mode under C_{3v} symmetry. In that case, the authors proposed that in some instances there is already a slight breakdown in the local symmetry due to the lower symmetry of the methylcyclopentadienyl ligand.[12] Clearly, the local symmetry of the $Mn(CO)_3$ moiety is susceptible to this kind of symmetry reduction. It should be noted that an interaction involving two of the three carbonyl groups also would lead to conditions of C_s symmetry and the same splitting pattern would be predicted.

An alternative explanation for the altered ν(CO) band profile upon adsorption is that the MMT is adsorbed on the surface in two different environments. Two unique chemical environments for the MMT should generate two different a_1 and *e* ν(CO) bands. It is possible that, since the a_1 mode is less sensitive to the chemical environment of the molecule than is the *e* mode, the two a_1 bands are coincident but the *e* modes are not. This could give rise to the number of bands observed in the CO stretching region (2150–1800 cm^{-1}).

In order to differentiate between these two possible explanations of the observed ν(CO) band profiles, a variable-loading experiment was performed using alumina (neutral, Grade I) as the surface. Alumina was chosen for this experiment because it was the substrate with the fewest peaks in the region of interest (2150–1800 cm^{-1}) and it perturbs the ν(CO) bands of MMT in a manner more similar to that of the soils than does silica. In this experiment, the amount of MMT adsorbed onto the alumina was controlled by varying the initial concentration of MMT present in solution. If the first scenario involving a symmetry breakdown is correct, the MMT loading on the surface should have no impact on the relative intensities of the components of the split *e* mode. However, the second scenario proposes that there are two different adsorption environments available on the surface. As it is unlikely that these two environments would produce identical stabilization energies upon adsorption of MMT, one site should be favoured over the other. If this were the case, varying the concentration of MMT on the surface should lead to a variation in the relative intensities of the two *e* modes, as the site offering the highest stabilization energy should be occupied first and only after saturation would the second site become occupied.

The results of the variable-loading experiment are presented in Fig. 3. Qualitatively, there is no variation of relative intensities between the two low-energy ν(CO) bands as the concentration of MMT on the alumina is varied by a factor of 10.

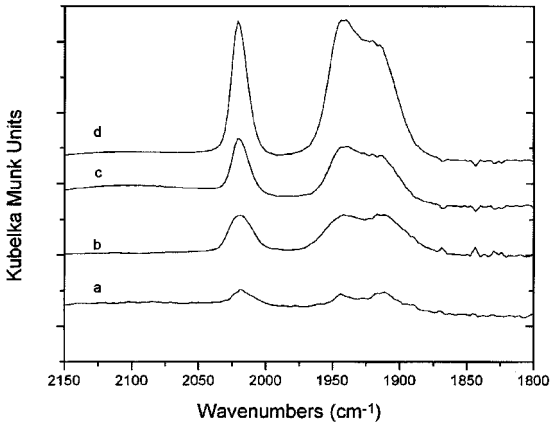

Figure 3 DRIFT spectra [ν(CO) region] of MMT adsorbed on neural alumina (a) 0.5%, (b) 2.7%, (c) 4.0% and (d) 7.0% w/w.

In order to examine this result quantitatively, the integrated intensities of the overlapping components of this ν(CO) band were obtained by peak fitting and are given in Table 3. Although they show some variability, the ratio of the integrated intensities of the two components of the *e* mode does not vary systematically with the loading of MMT on the alumina. Based on these results, the first scenario presented above is the more explanation for the observed splitting, namely that MMT undergoes some kind of interaction with the surface involving one or two of the carbonyl ligands. This leads to a breakdown in the local symmetry from C_{3v} to C_s and results in a splitting of the doubly degenerate *e* mode into an $a'(2)$ and an a'' mode.

Based on the conclusion that the *e* mode is being split by an interaction of the carbonyl group with the surface, a quantitative analysis of the MMT ν(CO) band envelope was undertaken. The peaks in the CO region (2150–1800 cm^{-1}) were band-fitted as described above. The MMT

Table 3 Integrated intensities of ν(CO) *e*-mode components of MMT

	Integrated intensity		
MMT loading (g MMT/g substrate)[a]	High-energy component	Low-energy component	Ratio
0.005	0.42	0.93	0.50
0.027	3.13	4.59	0.68
0.040	5.10	7.76	0.66
0.070	43.8	64.3	0.68

[a] Assuming all of the MMT was adsorbed.

Table 4 CO stretching frequencies of MMT

	ν(CO) (cm^{-1})		
Substrate	$a'(1)$	$a'(2)$	a''
ECSS8	2017.8	1940.6	1909.9
ECSS5	2016.5	1938.9	1898.8
ECSS4	2016.9	1938.4	1901.7
Topsoil	2015.2	1932.4	1912.6
Alumina	2018.8	1944.3	1911.9
Silica	2021.3	1946.3	1914.0

ν(CO) frequencies determined in this way are presented in Table 4. As observed for the CO bands in various solvents, the higher-energy, $a'(1)$ band, formerly the a_1 band under C_{3v} symmetry, is less sensitive to the chemical environment of the MMT, although it does show some small variations. For each of the soils, the $a'(1)$ mode varies between 2015.2 and 2017.8 cm^{-1}, whereas the same band is shifted to 2021.3 cm^{-1} when MMT is adsorbed onto silica. Alumina produces a more moderate shift to 2018.9 cm^{-1}. Comparison with the $a'(1)$ CO frequencies observed in various solvents (Table 2) suggests that the soils perturb this CO stretching mode by an amount analogous to that of a moderately coordinating solvent such as THF. Similarly, the $a'(1)$ CO frequency observed for silica suggests that it perturbs the CO stretching mode to a lesser degree, analogously to non-coordinating, non-polar solvents such as cyclohexane.

The ν(CO) *e* mode is much more sensitive to the chemical environment of the CO ligands and undergoes a lifting of its degeneracy. As described above, the *e* mode splits into an $a'(2)$ and an a'' band under C_s symmetry upon adsorption. The $a'(2)$ and a'' bands show a much larger dependence on the substrate than does the $a'(1)$ mode. ECSS4 and ECSS5 produce the largest frequency shifts and greatest splittings. The resulting $a'(2)$ and a'' bands for ECSS4 and ECSS5 are located at 1938.4 and 1901.7 cm^{-1}, and 1938.9 and 1898.9 cm^{-1}, respectively. ECSS8 exhibits a smaller shift, with the two bands appearing at 1940.6 and 1909.9 cm^{-1}. This is consistent with the small shift observed for the $a'(1)$ mode of MMT adsorbed on ECSS8. Topsoil also produces smaller shifts for the $a'(2)$ *and* a'' modes than do ECSS5 and ECSS4. The band positions observed on alumina are similar to those observed for ECSS8 and topsoil, while

the band positions on silica are at higher energy (1946.3 and 1914.0 cm^{-1}) than are those observed for any of the other substrates.

For all of the substrates, the *e* mode is split into an $a'(2)$ and an a'' mode with both of these bands remaining in the ν(CO) region (2150–1800 cm^{-1}). Therefore, the CO force constant associated with these CO stretching bands is still consistent with those observed for terminal carbonyl ligands in metal carbonyl complexes. This observation implies that interaction of the $Mn(CO)_3$ moiety with the soils and surfaces is not strong enough to decrease radically the bond strength of the C–O bond. Chemical adsorption can be classified by the type of bonding that can occur at an active site. Lewis active sites occur where a metal atom from the surface can act as an electron acceptor for the substrate. Brønsted sites occur where a surface hydroxyl group is available to form a hydrogen bond to the adsorbate.[14–16] Adsorption at a Brønsted site is typically weaker than is adsorption at a Lewis site and is often reversible. In contrast to Brønsted sites, Lewis adsorption usually involves chemical rearrangement and is not reversible.[17, 18] Lewis bonding between the metal carbonyl and the metal ions in the surface typically leads to strong interactions with the surface and produces more extreme changes in the CO region of the IR spectrum. Often these Lewis interactions give rise to ν(CO) bands below 1800 cm^{-1} indicative of a decreased CO bond order, due to the terminal oxygen bonding with the metal ion at the Lewis site.[19]

The interaction of MMT with the surfaces investigated in this work is most probably of the Brønsted type. In this case, a surface-bound hydroxyl group is capable of hydrogen bonding with the lone pairs on the terminal oxygens of the carbonyl ligands on MMT, as shown in Fig. 2. Hydrogen bonding would be a strong enough interaction to produce the observed symmetry breakdown from C_{3v} to C_s, leading to the splitting of the ν(CO) *e* mode. However, it would not be strong enough to alter radically the bond order of the CO ligand and thus would not give rise to CO bands below 1800 cm^{-1}.

As the proposed bonding site involves the hydroxyl functionality of the surface, an investigation into the effect of hydration and acidity of the surface was carried out. These experiments were performed using four grades each of neutral and basic alumina. The grade of the alumina was adjusted according to published methods.[10] The

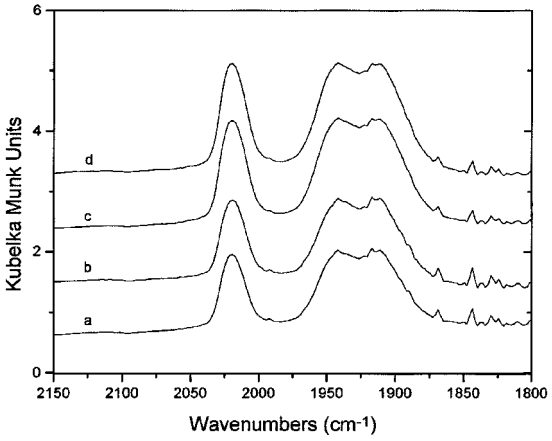

Figure 4 DRIFT spectra [ν(CO) region] of MMT adsorbed on basic alumina grades (a) II, (b) III, (c) IV and (d) V.

MMT was adsorbed onto the surfaces in the manner described above. The DRIFT spectra of MMT on different grades of basic and neutral alumina were obtained. The ν(CO) region of the DRIFT spectra of MMT on basic alumina is shown (Fig. 4). For both of the basic and neutral alumina, the $a'(1)$ mode appears at 2019 cm^{-1} and does not shift for grades II–V. The *e* mode is split as described above.

The CO bands were peak-fitted to detect any more suble changes in the band envelope due to the changes in the substrate. However, the peak positions, relative intensities and widths do not vary appreciably with hydration of the alumina surface. Furthermore, the parameters of the ν(CO) bands do not vary significantly between the neutral and basic alumina. These peak-fitting results are summarized in Table 5.

The fact that the ν(CO) parameters are unaffected by the grade and type of the surface would seem to be inconsistent with the fact that the binding site involves the hydroxyl functionality of the surface. However, all of the different grades include OH groups on the alumina surface. The drying conditions used to generate the various grades are not capable of producing anhydrous alumina. Since the MMT loading on the surface represents only a few per cent by weight, there should still be sufficient binding sites available on any of the substraes. The MMT binding should only be impacted at very high loadings. Unfortunately, high loading experiments, i.e. loadings which exceed the available number of binding sites, generate intense overlapping ν(CO) peaks that are too broad to

Table 5 Typical peak-fit results: ν(CO) modes of MMT on alumina

Type and grade	ν(CO) (cm^{-1}) $a'(1)$	$a'(2)$	a''	Intensity ratio, $a'(2)/a''$
Neutral grade II	2018.7	1944.2	1911.1	0.656
Neutral grade IV	2018.9	1945.0	1911.1	0.626
Basic grade II	2018.8	1944.3	1911.9	0.669
Basic grade IV	2018.6	1945.2	1911.2	0.678

analyse reproducibly.

To verify the reversibility of the interaction of MMT with the substrate, a desorption experiment was performed. A soil sample which had been washed with a solution of MMT, as above, was placed in an IR gas cell and evacuated (0.01 torr). After 18 h, the gas-phase IR spectrum of the headspace above the soil was acquired at medium resolution (4 cm^{-1}). Then the gas cell was heated by means of flowing glycerol at 75–80 °C around the inner jacket of the cell and a second-gas-phase IR spectrum was recorded. The gas-phase IR spectra obtained in this way are shown in Fig. 5 together with the gas-phase spectrum of MMT.

The CO stretching bands of MMT can be discerned at 2036.1 and 1959.7 cm^{-1} in each of the spectra. The rotational fine structure is not resolved in traces b and c because the spectra were acquired at 4 cm^{-1} resolution. However, upon closer examination of the peak shape, a shoulder can be seen at *ca* 2040 cm^{-1} which is consistent with the rotational fine structure observed in the high-resolution (0.11 cm^{-1}) spectrum of MMT (trace a). An interesting phenomenon can be seen adjacent to the CO stretching bands in spectrum (c) at 2020.7 and 1936.0 cm^{-1}. These features are hot bands resulting from transitions between the first vibrational excited state and the second excited state. This transition is observed at slightly lower energy than the fundamental because of the anharmonicity of the potential well.[20] As the temperature increases, the hot bands increase in intensity as the populations of the excited vibrational states increase. For the high-resolution gas-phase spectrum of MMT no hot bands are observed, as the spectrum was acquired at a lower temperature.

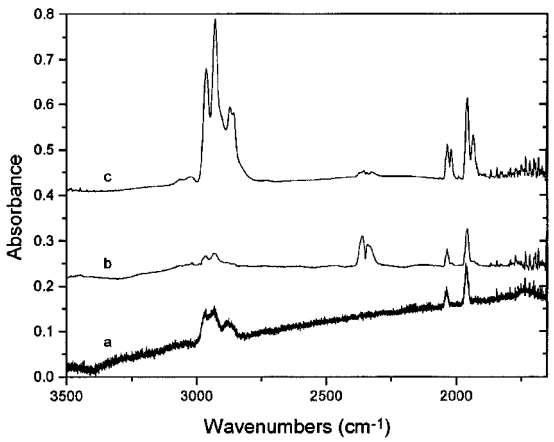

Figure 5 Gas-phase IR spectra: (a) high-resolution, MMT sample; (b) headspace above MMT-treated soil after 18 h; (c) sample from (b) heated to 75–80 °C.

In all three of the spectra presented in Fig. 5, a number of bands between 3100 and 2850 cm^{-1} are also visible. These are the expected C–H stretches of the methylcyclopentadienyl ligand. The bands at 2964 and 2933 cm^{-1} have been assigned to the a'' and a' modes of the CH_3 substituent on the ring under C_s local symmetry.[12] The bands above 3000 cm^{-1} have been observed previously but have not been assigned.[13] They are typical of C–H stretches of conjugated cyclic ligands such as the methylcyclopentadienyl ring. These bands and the CO bands clearly indicate that gas-phase MMT is evolving from the soil. The desorption of MMT from the soil under these relatively mild conditions suggests a weak, reversible interaction between the adsorbate and the substrate. Such an interaction is consistent with the proposed Brønsted binding site for MMT on the soil.

In this study and in previous work,[8] MMT has been shown to be stabilized by adsorption. An interaction between MMT and a substrate, such as the proposed Brønsted interaction with inorganic clay-type site (Fig. 2), would allow the

substrate to act as an electron sink. Photo-ejection of a CO ligand is generally accepted as the first step in the decomposition of MMT as well as other, similar organometallic compounds.[21, 22] By inhibiting this decomposition pathway, the environmental half-life of MMT could be increased significantly, as has been observed in a previous study in our laboratory.[8] If the substrate accepts electron density from the terminal oxygen of the carbonyl ligand, the strength of the Mn–C bond is altered. This could shift the UV–visible absorbance profile and inhibit photo-ejection of the CO ligand. Alternatively, since the substrates are opaque to UV–visible radiation, MMT adsorbed on the interior of the porous material could be shielded from decomposing radiation.

Conclusions

MMT has been shown, using DRIFTS, to adsorb to a variety of soils and materials. In each case, the ν(CO) region (2150–1800 cm^{-1}) of MMT is altered upon adsorption to a substrate. The frequency shifts of the CO stretching modes and the symmetry breakdown of the $Mn(CO)_3$ moiety suggest an interaction involving one or two of the three carbonyl ligands. The absence of CO stretching bands below 1900 cm^{-1} indicates that the interaction does not involve Lewis bonding. Furthermore, the ready desorption of MMT from the soils under vacuum, as determined by the gas-phase headspace IR experiments, indicates that the interaction is reversible. This evidence supports the proposed Brønsted binding site shown in Fig. 2. This Brønsted interaction with a soil could stabilize MMT in a number of different ways by reducing the potential for photo-ejection of a carbonyl ligand. Inhibition of this decomposition pathway could explain the observed longevity of MMT adsorbed on soils.

REFERENCES

1. A. B. Callear and R. G. W. Norrish, *Proc. R. Soc., London, Ser. A* **259**, 304 (1960).
2. M. E. Meek and R. Bogoroch, *Methylcyclopentadienyl Manganese Tricarbonyl: An Assessment of the Human Health Implications of its Use as a Gasoline Additive*, Environmental Health Directorate, Health Protection Branch, Ministry of National Health and Welfare, Ottawa, Canada, 1978, and references therein.
3. M. Hotz, *Alternatives to Lead in Gasoline: The Commission on Lead in the Environment*, Royal Society of Canada, Ottawa, Canada, 1986.
4. PRNewswire Service, 14 April 1995; 13 July 1995; 20 Oct. 1995; 28 Nov. 1995; 8 March 1996. Source: Comtex Scientific Corporation.
5. P. J. Abbott, *Sci. Tot. Environ.* **67**, 274 (1987).
6. D. K. Hysell, W. Moore, J. F. Stara, R. Miller and K. I. Campbell, *Environ. Res.* **7**, 158 (1974); R. P. Hanzlik, R. Stitt and G. J. Traiger, *Toxicol. Appl. Pharmacol.* **56**, 353 (1980).
7. G. L. Ter Haar, M. Griffing, M. Brandt, D. Oberding and M. Kapron, *Air Pollut. Control Assoc.* **25**, 858 (1975).
8. A. J. Vreugdenhil and I. S. Butler, *Appl. Spectrosc.* **49**, 482 (1995).
9. J. Mink, *Mikrochim. Acta* **3**, 63 (1987).
10. A. Gordon and R. Ford, *The Chemist's Companion*, Wiley–Interscience, New York, 1972.
11. D. W. Marquardt, *J. Soc. Ind. Appl. Math.* **11**, 431 (1963).
12. D. J. Parker, *Spectrochim. Acta* **31A**, 1789 (1975).
13. L. T. Reynolds and G. Wilkinson, *J. Inorg. Nucl. Chem.* **9**, 86 (1959); L. M. C. Shen, G. G. Long and C. G. Moreland, *J. Organometal. Chem.* **5**, 362 (1966); R. D. Fisher, *Chem. Ber.* **93**, 165 (1960).
14. J. B. Peri, *J. Phys. Chem.* **69**, 220 (1965).
15. J. B. Peri and R. B. Hannan, *J. Phys. Chem.* **64**, 1526 (1960).
16. A. V. Kiselev and V. I. Lygin, *Infrared Spectra of Surface Compounds*, John Wiley, New York, 1975.
17. A. Zecchina, E. E. Platero and C. O. Arean, *J. Mol. Catal.* **45**, 373 (1988).
18. Bagshaw and R. P. Cooney, *Appl. Spectrosc.* **50**, 310 (1996).
19. A. Kazusaka and R. F. Howe, *J. Mol. Catal.* **9** 183 (1980).
20. N. B. Colthup, L. H. Daly and S. E. Wiberley, *Introduction to Infrared and Raman Spectroscopy* 3rd edn, Academic Press, Boston, 1990, pp. 15–31.
21. P. S. Braterman and J. D. Black, *J. Organometal. Chem.* **39**, C3 (1972).
22. T. E. Bitterwolf, K. A. Lott, A. J. Rest and J. Mascetti, *J. Organometal. Chem.* **419**, 113 (1991).

